

Article

Evaluating the Effect of Noise from Traffic on HYB Magnetic Observatory Data during COVID-19 Lockdown

Manjula Lingala *, Phani Chandrasekhar Nelapatla  and Kusumita Arora

Geomagnetic Observatories, CSIR-National Geophysical Research Institute, Uppal Road, Hyderabad 500007, India; phani@ngri.res.in (P.C.N.); karora@ngri.res.in (K.A.)

* Correspondence: manjulal.1118@ngri.res.in

Abstract: Continuous time series data from geomagnetic observatories are increasingly contaminated by anthropogenic noise related to developing socio-economic activities. More and more sophisticated techniques of data processing are used to eliminate this noise; nonetheless, some of it cannot be removed. The main sources of noise in the Hyderabad (HYB) data are vehicular traffic, power lines and a power station, 500 m to 1 km away. During the nationwide COVID-19 pandemic lockdown from 24 March to 17 May 2020, both road and metro rail traffic came to a complete halt. The data from this time interval give us an opportunity to evaluate the effects of the absence of traffic-generated noise sources. We found noticeable differences in the noise levels present in vector and scalar variation data, due to the vehicular noise observed before and during the lockdown periods. Noise spectrum estimates quantify the reduction in the noise levels during this period. We also noticed decreased scatter in absolute values of the H (horizontal), D (declination), Z (vertical) and I (inclination) components of the geomagnetic field during lockdown. The details of increased data quality in the absence of traffic-generated noise sources are discussed.

Keywords: geomagnetic vertical component; total field component; COVID-19 lockdown; vehicular traffic; noise levels



Citation: Lingala, M.; Nelapatla, P.C.; Arora, K. Evaluating the Effect of Noise from Traffic on HYB Magnetic Observatory Data during COVID-19 Lockdown. *Appl. Sci.* **2022**, *12*, 2730. <https://doi.org/10.3390/app12052730>

Academic Editor: Youngmin Kang

Received: 16 December 2021

Accepted: 30 January 2022

Published: 7 March 2022

Publisher's Note: MDPI stays neutral with regard to jurisdictional claims in published maps and institutional affiliations.



Copyright: © 2022 by the authors. Licensee MDPI, Basel, Switzerland. This article is an open access article distributed under the terms and conditions of the Creative Commons Attribution (CC BY) license (<https://creativecommons.org/licenses/by/4.0/>).

1. Introduction

Continuous measurements at geomagnetic observatories are a very important source for understanding short-term and long-term changes in the geomagnetic field, both due to variations in the Earth's interior and the near-Earth environment. Across the globe, 153 INTERMAGNET observatories are providing uninterrupted measurements of vector and scalar components of the Earth's magnetic field, and the Hyderabad Magnetic Observatory (HYB) is one among them. Further advances in studies of the internal and external field in combination with data from satellites requires much higher accuracies and resolution of data. Monitoring the geomagnetic field is of crucial importance in today's technology-dependent world (e.g., for satellite health and telecommunication systems).

Disturbances in the magnetic measurements from electrical railways have previously been studied; theoretical calculations of the magnetic field values generated by DC railway cars have been developed [1,2]. Ref. [3] studied disturbances in geomagnetic measurements at BJI Observatory, caused by direct current (DC) railway systems, and proposed a noise reduction method based on the adaptive Kalman filter. Disturbances from power lines in the magnetic data have been identified and quantified by [4–6]. Ref. [7] reported and rectified different sources of anthropogenic noise due to heavy vehicle movements, power fluctuation problems, etc. Ref. [8] reported perturbances in the Easter Island observatory, produced by trucks' movements at a stone quarry located near to the observatory campus, and also due to the movement of airplanes 100 m away from the measurement site. Ref. [9] performed a detailed analysis on the factors that affect total field measurements.

To meet the international standards, observatory staff make meticulous efforts to deliver a good quality geomagnetic time series data by using algorithms to detect and

remove the noise in HYB Observatory data caused by the metro line, based on its structural stability. The algorithm works as follows: when a change in dZ between neighboring measurements (in absolute value), exceeding a given threshold, is found, three subsequent measurements are discarded. It is clear that this algorithm creates the following risks: (a) natural signals with sharp edges, for example, during magnetic disturbances, may be discarded; (b) noise may be incompletely removed if its duration is long; (c) noise can be missed if, due to a small shift, its leading edge takes two samples. However, to calculate the minute values of magnetic field variations, this may be enough [7]. Representing the natural field variations is becoming a challenging task, due to increased construction, public transportation and development activities around the magnetic observatories, which has become a source of degradation of magnetic data quality. The parameters that affect the data quality depend on the instrument characteristics, data resolution, expertise of the observer and characteristics of the geomagnetic field, defined by the specific location of a magnetic observatory. Such parameters could be natural (temperature, humidity, groundwater circulation, telluric currents, frequency of lightning, magnetic gradient, etc.) or man-made (AC and DC sources in the vicinity of the sensor, sensor alignment, time stamping, etc.). Due to the increase in urban expansion, as well as the infrastructural facilities in cities, producing good quality and highly accurate geomagnetic measurements by cleaning the artificial noise is increasingly difficult, even though the observatories were originally built in magnetically quiet locations. In this context, to maintain good data quality, it is necessary to understand and assess the factors associated with changing environmental day-to-day conditions that influence data quality, so as to improve the data acquisition and processing procedure accordingly.

During the COVID-19 pandemic situation, the INTERMAGNET Hyderabad Observatory has committed to continue its operations in recording the Earth's magnetic field without any interruption even with very limited staff during the nationwide lockdown in India (from 24 March to 17 May 2020). An attempt is made to identify and characterize the anthropogenic noise due to metro rail services and vehicular traffic on the 1s data quality of vector and scalar magnetic measurements at HYB.

2. Data and Results

In order to achieve the aim of the study, we studied and analyzed the 1 Hz vector variation HDZ data acquired from a tri-axial fluxgate magnetometer and the 1 Hz scalar variation (F) data acquired from a GSM90-F1 magnetometer for 50 days before and 50 days during lockdown (1 February to 10 May 2020). Quiet days were chosen in March (before lockdown) and compared with April 2020 (during lockdown) for the analysis. Further, we used the vector and scalar data from the Choutuppal (CPL) Magnetic Observatory of this institute, 65 km away from HYB, for comparison. The CPL Observatory is located in a 100 acre campus, and is relatively far from sources of anthropogenic and cultural noises.

International quiet (IQ) days vary from the highest to the lowest order of quietness and disturbance, respectively [10]. This classification leads to the study of the different physical processes in the ionosphere and magnetosphere, which cause variations in the geomagnetic field. The K-index is defined as a quasi-logarithmic measure, ranging in steps of one, from zero to nine, of the range of geomagnetic disturbance at a geomagnetic observatory in a three-hourly UT interval (00–03, 03–06, . . . , 21–24) [1]. The K-sum is the sum of all 3 h interval K-index values of one day. The IQ days of March 2020 were 14, 11, 5, 10 and 7 prior to lockdown (K-sum was 4, 4, 8, 7 and 6, respectively), and in April 2020, they were 30, 29, 06, 23 and 17 during lockdown (K-sum was 1, 3, 3, 5 and 5, respectively). The diurnal geomagnetic field variations in H, D, Z and F (for quiet days, 11 March (DoY 71) and 6 April 2020 (DoY 97)) are shown in Figure 1 (top and bottom panel).

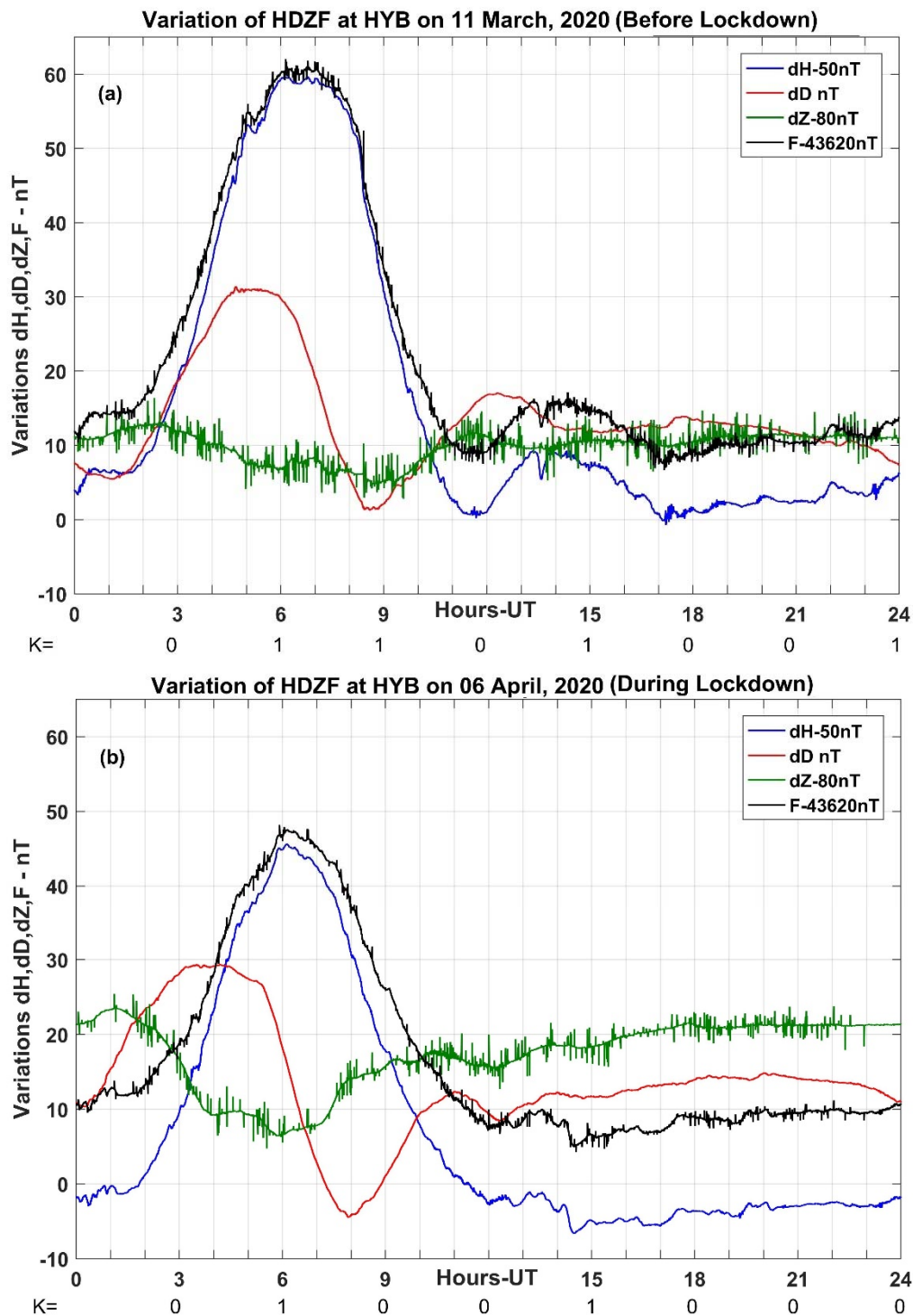


Figure 1. Diurnal variation in H, D, Z and F on one of the best quiet days of the respective months along with their K-index values, on (a) 11 March 2020 (before lockdown) and (b) 6 April 2020 (during lockdown). For plotting convenience, dH, dZ and dF are subtracted by 50 nT and 80 nT and 43,620 nT, which represent the deviation in 1 Hz value data from the base values.

In Figure 1, the top panel indicates the raw variations in the geomagnetic field at HYB (vector and scalar) on quiet days before lockdown, i.e., 11 March 2020, and the bottom panel indicates the data during lockdown, i.e., 6 April 2020. Blue and red colors indicate the H and D components. Visually, it appears that there is no significant change in data quality before and during lockdown. The green and black lines indicate the Z and F components'

variation data. Comparing the Z and F components before and during lockdown periods shows a visibly reduced frequency of noise peaks during lockdown. We also noticed spikes with an amplitude of around 7 nT in the Z and F components in the period before lockdown, whereas an amplitude of around 4 nT is observed during the lockdown period.

The maximum amplitude of first difference is ± 0.2 nT in the H and D components both before and during lockdown, while it is ± 4 nT in Z before lockdown, which is reduced to ± 3 nT during lockdown (Figure 2, top panel in green). The spikes with an amplitude between 3 and 4 nT are reduced by eight times in the lockdown period, when compared to before lockdown. Similarly, the amplitude of spikes between 1 and 3 nT in the lockdown period are reduced by half when compared to before lockdown. The maximum amplitude of first difference of the F component is noted as ± 2 nT, both before and during lockdown. The range of first difference values in each component is independent of the magnetic activity levels. Additional case studies for before and during lockdown are provided in Figures S1 and S2 in the Supplementary Information.

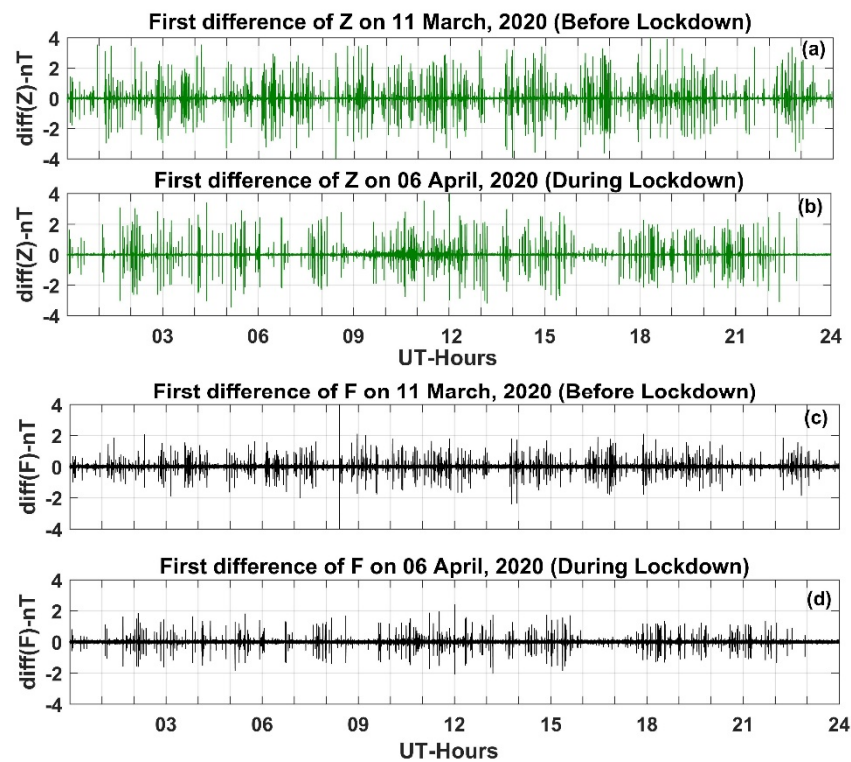


Figure 2. Shows the first difference (the approximate derivative) of 1s measurements of Z and F components. (a) Z component on 11 March 2020 (before lockdown), (b) Z component on 6 April 2020 (during lockdown), (c) F component on 11 March 2020 (before lockdown) and (d) F component on 6 April 2020 (during lockdown).

We also tried to assess whether the reduction in noise during lockdown affected the quality of absolute measurements. These absolute observations are performed manually on a weekly basis using a DI single-axis fluxgate magnetometer, producing spot values of D and I specific to a time at that location. Simultaneous scalar-F measurements are also carried out during the period of D/I observations, from which the absolute values of the H, D and Z components are derived. Figure 3 shows the absolute values of D, I and F from February 2020 to May 2020. The red color depicts the spot values from before lockdown and the green color depicts those during lockdown. Some variations in spot values can be ascribed to the different times of day at which measurements were performed. Overall, the I and F spot values are more consistent compared to D. Scatter between the absolute measurements of D, I and F carried out on the same day ranges from 0.05 to 0.5 min, 0.03 to

0.1 min and 0.6 to 3.6 nT, respectively, before lockdown, and 0.07 to 0.6 min, 0.02 to 0.5 min and 0.6 to 2.1 nT during lockdown.

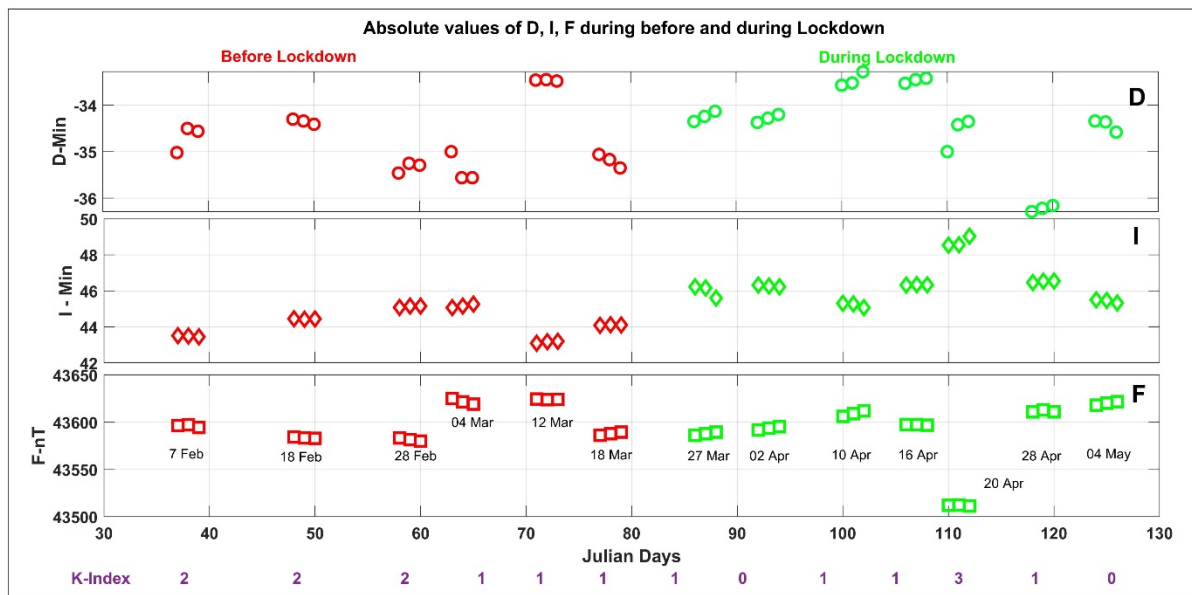


Figure 3. Absolute values of D, I and F components before (7 February 2020 to 18 March 2020, red color symbols) and during (27 March 2020 to 4 May 2020, green color symbols) the lockdown period, with annotation of dates of observations and K-index value during the time the observations were conducted.

These absolute measurements were used to calculate the baselines of H, D and Z, which are necessary to prepare definitive data of the geomagnetic field components. Having assessed the amplitudes of noise in the variation data and absolute measurements of D and I, we checked the effect on the calculated baselines (only for 86 days, including the lockdown period). These baselines were processed by only considering those spot values of absolute and variation data, which are consistent and devoid of noise, and excluding data points that have high noise levels during the period of observation. In Figure 4, the left side (red) portion indicates the baselines of H, D and Z before lockdown and the right side (green) is during the lockdown period. Over the observation period (45 days), the baseline variation range was about 0.6 nT, 0.06 min and 0.4 nT in the H, D and Z components, respectively, before lockdown. During the period of lockdown (42 days), the corresponding values changed slightly to 0.4 nT, 0.05 min and 0.8 nT, respectively. The standard deviations of measurements from the calculated baselines reduced by 25–50% in the different components during the lockdown period, compared to normal traffic conditions, as shown in Table 1. The averages of the differences in amplitudes between consecutive values of calculated baselines for each day of absolute measurement were 0.29 nT, 0.05 min and 0.13 nT for H_B , D_B and Z_B before lockdown, and 0.24, 0.03 and 0.17 during lockdown, showing that the baselines were undisturbed by the vehicular noise, as shown in Table 2.

Table 1. Details of geographic and geomagnetic dipole coordinates (GDC) of the HYB and CPL Observatories used in the study.

	HYB	CPL
Established on	1965 by CSIR-NGRI	2012 by CSIR-NGRI
Geographic Latitude	17°25.0' N	17°17.6' N
Geographic Longitude	78°33.0' E	78°55.2' E
Geomagnetic dipole Latitude	09°00.0' N	08°49.2' N

Table 1. Cont.

	HYB	CPL
Geomagnetic dipole Longitude	152°13.2' E	152°36.0' E
Local Time	UT + 05:30 h	UT + 05:30 h
Year of INERMAGNET status	2009	2019

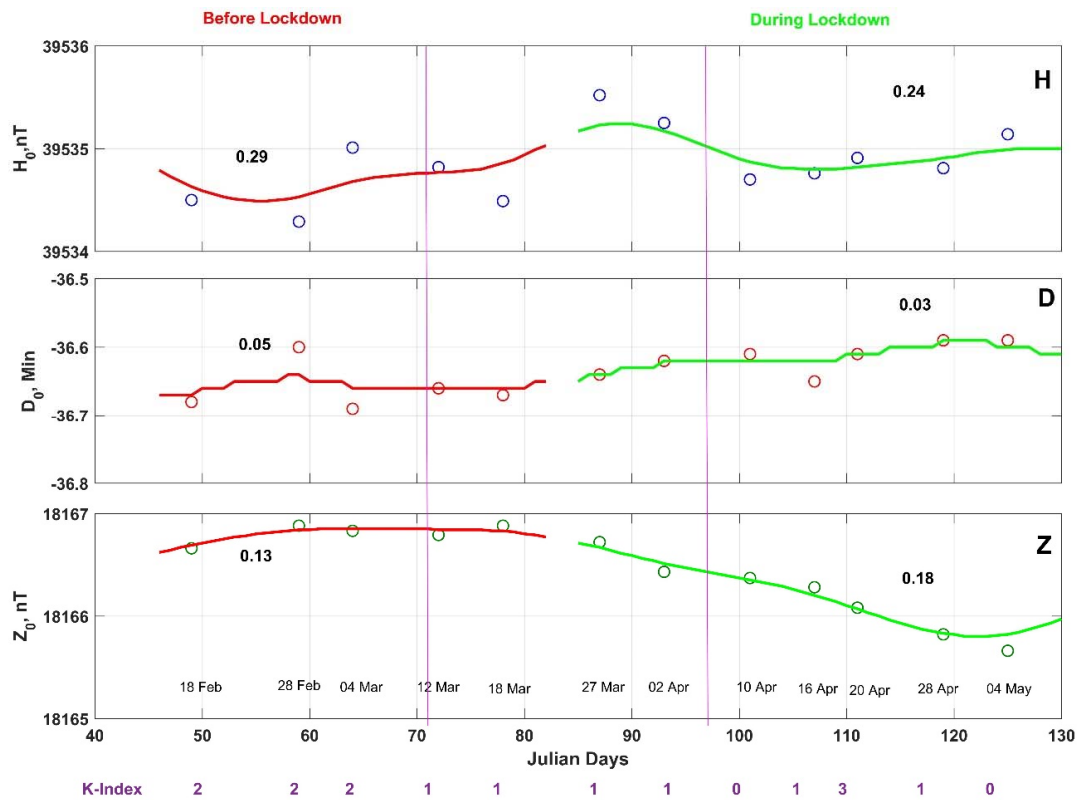


Figure 4. HDZ baselines observed (circles) and adopted (line) along with their scatter value before (7 February 2020 to 18 March 2020, red color line) and during (27 March 2020 to 4 May 2020, green color line) the lockdown period, with annotation of dates of observations and K-index value during the time the absolute observations were conducted. Pink vertical lines indicate the dates of diurnal variations, as shown in Figure 1.

Table 2. Values of baselines, average and standard deviation before and during lockdown.

Date	H _B (nT)	D _B (min)	Z _B (nT)	δ H	δ D	δ Z
07.02.2020	39,534.5	−36.68	18,166.4			
18.02.2020	39,534.5	−36.68	18,166.6	−0.01	0	0.26
28.02.2020	39,534.3	−36.60	18,166.9	−0.21	0.08	0.22
04.03.2020	39,535.0	−36.69	18,166.8	0.72	−0.09	−0.05
12.03.2020	39,534.8	−36.66	18,166.8	−0.19	0.03	−0.04
18.03.2020	39,534.5	−36.67	18,166.9	−0.33	−0.01	0.09
Average of variable amplitudes				0.29	0.05	0.13
Standard deviation of variable amplitudes				0.42	0.06	0.14
27.03.2020	39,535.5	−36.64	18,166.7			
02.04.2020	39,535.2	−36.62	18,166.4	−0.27	0.02	−0.29

Table 2. *Cont.*

Date	H _B (nT)	D _B (min)	Z _B (nT)	δ H	δ D	δ Z
10.04.2020	39,534.7	−36.61	18,166.4	−0.55	0.01	−0.06
16.04.2020	39,534.8	−36.65	18,166.3	0.06	−0.04	−0.09
20.04.2020	39,534.9	−36.61	18,166.1	0.15	0.04	−0.2
28.04.2020	39,534.8	−36.59	18,165.8	−0.1	0.02	−0.26
04.05.2020	39,535.1	−36.59	18,165.7	0.33	0	−0.16
Average of variable amplitudes				0.24	0.03	0.18
Standard deviation of variable amplitudes				0.32	0.03	0.09

3. Noise Characteristics

We calculated the noise spectra in the HYB data and identified the outliers, which will provide information about the deviation of these points from the mean value. With the available information from the outliers, we designed a zero-phase forward low-pass Butterworth filter of order six, with a cut-off frequency 0.01 Hz, to eliminate the noise in the Z and F components of the HYB raw data.

Figures 5 and 6 show the details of the raw and filtered data before and during the lockdown period from the HYB Observatory. From Figures 5a,b,f,g and 6a,b,f,g, a noticeable difference is observed in the occurrence frequency of spikes in the Z and F components before and during the lockdown period. Even though the amplitude was found to be in the range of ± 2.5 nT in the Z and F components, the density distribution and frequency of spikes were significantly reduced in the lockdown period when compared to before lockdown. A frequency peak was observed in the noise spectra at 11 mHz in the Z and F components before lockdown and during the lockdown period, and the same frequency peak was noticed with reduced power intensity during the lockdown period in both the components (Figures 5c,h and 6c,h). Figures 5d,i and 6d,i show the raw signal after removing the noise with a low-pass Butterworth filter with a lower cut-off frequency of 0.01 Hz in the Z and F components. Figures 5e,j and 6e,j show the 1 Hz raw signal of the Z and F components from the CPL Observatory. Comparing Figure 5d,i with Figure 5e,j, and Figure 6d,i with Figure 6e,j, shows that the filtered data are consistent with the raw data from CPL, after removing the remaining sources of anthropogenic noise on the Z and F components at the HYB Observatory.

We also attempted to identify the effect of vehicular noise on the H and D components from the HYB Observatory before and during the lockdown period, and our analysis shows that a negligible difference was observed in the occurrence frequency of spikes, both in the H and D components, before and during the lockdown period, within the range of ± 0.03 nT. As observed in the Z and F components, we also observed peaks in the noise spectra at 11 mHz in the H and D components during and before the lockdown period at the HYB Observatory. We also compared the 1 Hz trends of the HYB H and D components with CPL and found that these trends are consistent.

To strengthen our observations with the filtered data for the Z and F components from HYB, we subtracted the corresponding variations from CPL for the days before and during lockdown periods, and the linear trend shows good synchronicity between the observatories. Further, a small deviation of 1.5 nT was observed from the zero crossing line in all the components, which could be due to the distance between the observatories, followed by different geological constraints.

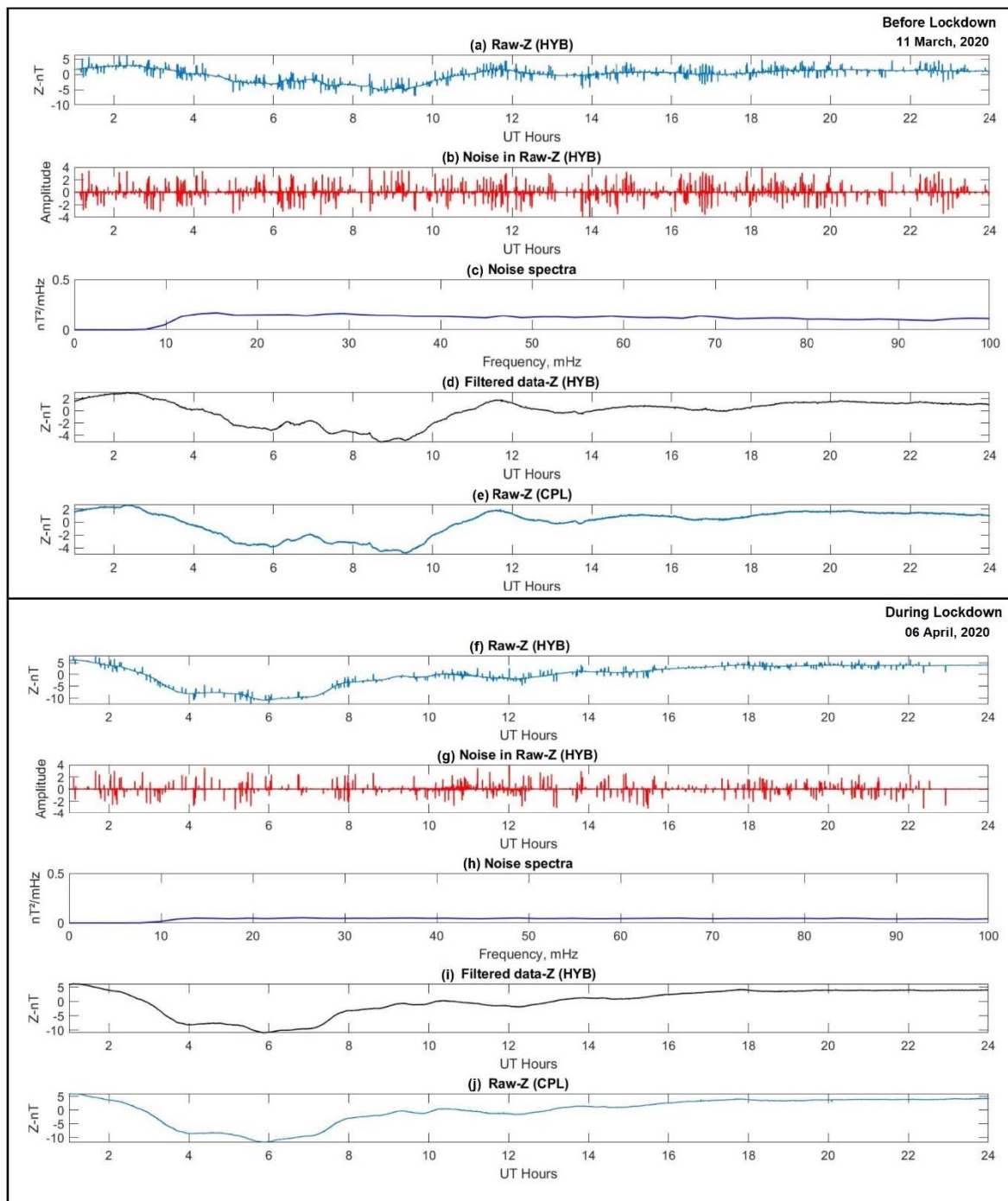


Figure 5. Plots of HYB 1 Hz Z component data before the lockdown period: (a) raw data; (b) noise in the data; (c) noise spectra; (d) filtered data; (e) CPL raw data of Z component. Plots of HYB 1 Hz Z component data during the lockdown period: (f) raw data; (g) noise in the data; (h) noise spectra; (i) filtered data of Z component; (j) CPL raw data of Z component.

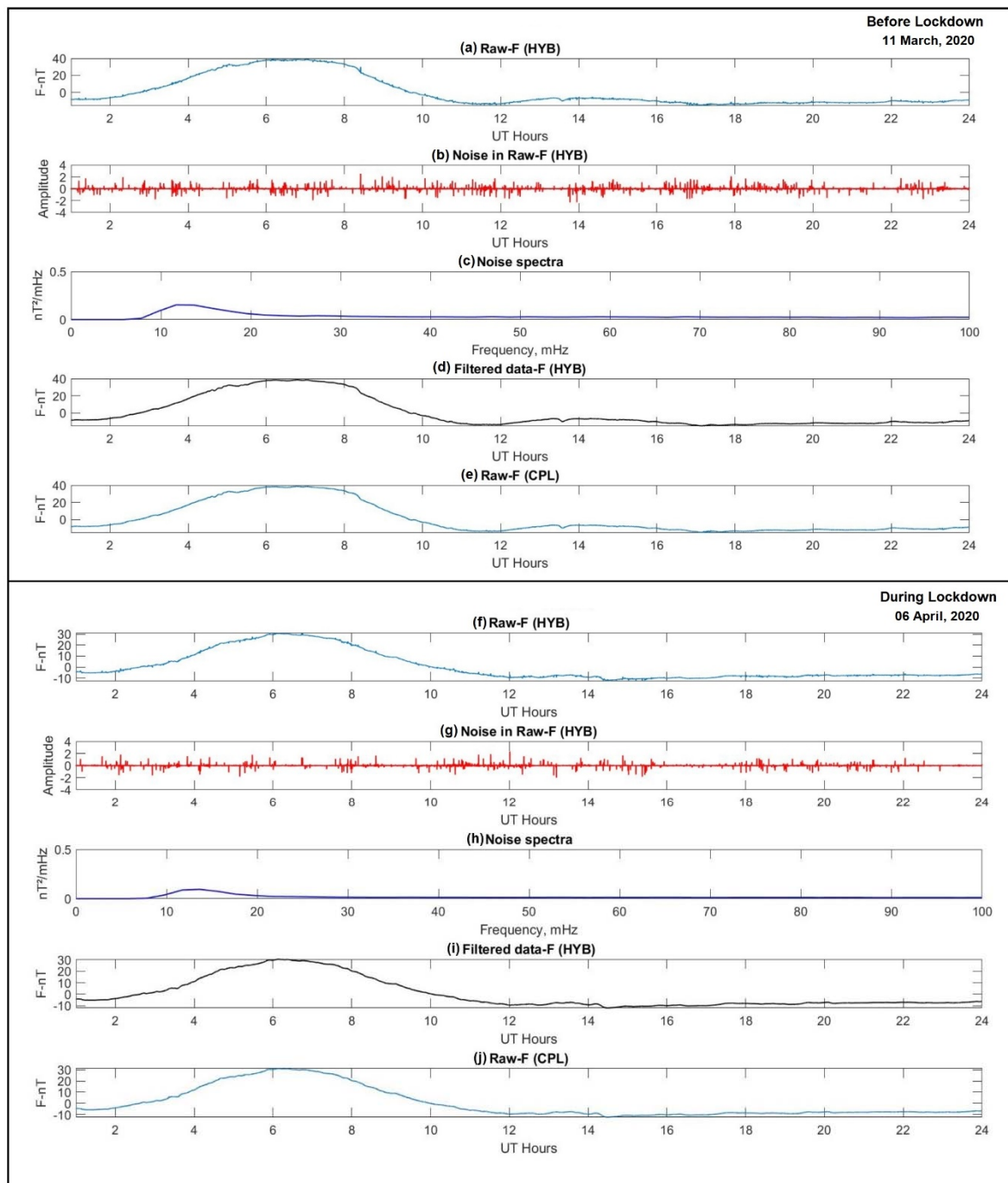


Figure 6. Plots of HYB 1 Hz F component data before the lockdown period: (a) raw data; (b) noise in the data; (c) noise spectra; (d) filtered data; (e) CPL raw data of F component. Plots of HYB 1 Hz F component data during the lockdown period: (f) raw data; (g) noise in the data; (h) noise spectra; (i) filtered data of F component; (j) CPL raw data of F component.

4. Discussion

To estimate the influence of vehicular noise on the 1 Hz measurements of the Z and F data at the HYB Observatory, we analyzed 100 days of data before and during lockdown. Raw variations in Z and F before and during lockdown showed quantifiable differences in the noise levels, with a reduction, to more than half, in the occurrence frequency of spikes. The spike amplitudes of first differences reduced from ± 4 nT before lockdown to ± 2.5 nT during lockdown in both Z and F.

A noticeable difference is observed in the occurrence frequency of spikes and the distribution density of spikes, which decreased in both the Z and F components during the lockdown period. We observed that the noise had an amplitude of about 8 nT in the raw data of the Z and F components before lockdown and 4 nT during lockdown, when there was no vehicular movement or metro rail. Similarly, at the KEL station (South Moravia), which is 25 m away from the local street, 5–10 nT spikes in the data were observed, attributable to the vehicle movements. Spike amplitudes increase for vans and buses; furthermore, a clear correlation between the spikes and traffic is established by experimental recording using another instrument placed 5 m away from the variometer and closer to the street [11]. Ref. [12] reported that at the EBR Observatory (Spain), which was located 0.5 km away from the railway, there were perturbations of about 3 nT and 15 nT in the H and Z components, similar to the effects of anthropogenic noise in the Z component noticed at HYB. In addition, comparing the EBR data with the SPT and AQU stations, which are located in noise-free places, 100 km and 200 km from EBR, respectively, magnetic disturbances appear in the EBR data, but not at the other two observatories, and are statistically estimated to be 89% due to train movements and 11% due to other sources. Similarly, at HYB, the noise was reduced by 60% during lockdown, in the complete absence of metro rail and all vehicular movement; the remaining 40% of noise would be due to the power lines and power station, which are at a distance of 500 m–1 km.

Ref. [6] identified the influence of two DC power lines, Baltic Cable, operated by Baltic Cable AB, and Kontek, operated by Energinet (<https://en.energinet.dk/>) (accessed on 27 November, 2021), on magnetic H and Z elements at Brorfelde (BFE) Geomagnetic Observatory, and found that the H component is increased by about 0.0040 nT per megawatt of increased power by Baltic Cable, and about 0.0022 nT per ampere of increased current by Kontek Cable. The Z component is decreased by about 0.0013 nT for every megawatt of power increase at Baltic Cable, and by about 0.0016 nT for every ampere of current increase at Kontek Cable. Ref. [8] discussed the noise signatures of planes in the geomagnetic data during take-offs and landings (for a few minutes noticed perturbances in the geomagnetic measurements about a few nT) which was about 100 m away from the new Easter Island observatory located at the end of Mataverí airport.

Ref. [13] identified the noise in the Duronia (DUR) Observatory data during 2018 by computing the signal-to-noise ratio (SNR) on hourly averaged power spectra of both horizontal components (H and D). The observed noise peak at DUR during morning hours was ascribed to the contribution of Pc3–Pc4, as well the contribution of higher levels of local noise in the data. Therefore, the observed peak at 11 mHz in the Z and F components during and before the lockdown periods (Figures 5c,h and 6c,h), as well as in the H and D components (not shown here) at the HYB Observatory, is probably due to the presence of residual signal (noise + ULF waves), which is a well-known behavior in the frequency range Pc3–4 (7–100 mHz). The contribution of these two components is difficult to discriminate.

5. Conclusions

- The observed spikes in the Z and F components is reduced by eight times in the lockdown period (in the absence of vehicular and metro rail traffic), with amplitudes between 3 and 4 nT, when compared to before lockdown.
- There was no obvious effect of lockdown on the D and I absolute measurements.
- The differences between the average of variable amplitudes and standard deviation of D_B , H_B , and Z_B before and during lockdown were very small, 0.02 min, 0.05 nT and 0.05 nT, and $\delta D \leq 0.03$ min, $\delta H \leq 0.1$ nT and $\delta Z \leq 0.05$ nT, respectively. There was not much difference in D_B , H_B and Z_B during lockdown.

Supplementary Materials: The following supporting information can be downloaded at: <https://www.mdpi.com/article/10.3390/app12052730/s1>, Figure S1: Diurnal variation of HDZ & F along with K-index values on 07, 10, 14 March (left) and 17, 19, 29 April 2020 (right) are best quiet days of the respective months. For plotting convenience dH, dZ and dF are subtracted by 50 nT and 80 nT and 43620 nT.; Figure S2: Shows first difference of 1-second measurements of Z and F. (a) First difference

of Z-component on 07, 10, 14 March, 2020 (before lockdown) (b) First difference of Z-component on 17, 19, 21 April, 2020 (during lockdown) (c) First difference of F-component on 07, 10, 14 March, 2020 (before lockdown) (d) First difference of F-component on 17, 19, 21 April, 2020 (during lockdown).

Author Contributions: Conceptualization and Methodology: M.L., P.C.N. and K.A.; Writing—original draft preparation: M.L. and P.C.N.; Writing—review and editing and overall supervision: K.A. All authors have read and agreed to the published version of the manuscript.

Funding: This research received no external funding.

Informed Consent Statement: Not applicable.

Data Availability Statement: HYB Observatory 1 Hz data used for this study are available at Institutional repository of CSIR-NGRI http://ngri.org.in/upload/kusumita/NGRI_respiratory_MDPi.zip (accessed on 2 November 2021).

Acknowledgments: The authors would like to thank the Director of the CSIR-National Geophysical Research Institute for the permission to publish this work; contribution no. NGRI/Lib/2021/Pub-161. We thank the Editor and anonymous reviewers for the careful reading of our manuscript and insightful comments and suggestions, which have improved the structure and the standard of the manuscript.

Conflicts of Interest: The authors declare no conflict of interest.

References

1. Pirjola, R.; Newitt, L.; Boteler, D.; Trichtchenko, L.; Fernberg, P.; McKee, L.; Danskin, D.; Jansen van Beek, G. Modelling the disturbance caused by a dc-electrified railway to geomagnetic measurements. *Earth Planets Space* **2007**, *59*, 943–949. [[CrossRef](#)]
2. Lowes, F.J. DC railways and the magnetic fields they produce—The geomagnetic context. *Earth Planets Space* **2009**, *61*, i–xv. [[CrossRef](#)]
3. Ding, X.; Li, Y.; Wu, Y.; Duan, S.; Li, Z.; Yin, Y.; Pan, L. A reduction method for magnetic disturbance caused by DC railway system. *Earth Planets Space* **2021**, *73*, 107. [[CrossRef](#)]
4. Wienert, K.A. *Notes on Geomagnetic Observatory and Survey Practice*; Series: Earth Sciences; UNESCO: Paris, France, 1970; 217p.
5. Jankowski, J.; Sucksdorff, C. *Guide for Magnetic Measurements and Observatory Practice*; IAGA: Warsaw, Poland, 1996; 235p.
6. Fox Maule, C.; Thejll, P.; Neska, A.; Matzka, J.; Pedersen, L.W.; Nilsson, A. Analyzing and correcting for contaminating magnetic fields at the Brorfelde geomagnetic observatory due to high voltage DC power line. *Earth Planets Space* **2009**, *61*, 1233–1241. [[CrossRef](#)]
7. Khomutov, S.Y.; Mandrikova, O.V.; Budilova, E.A.; Arora, K.; Manjula, L. Noise in raw data from magnetic observatories. *Geosci. Instrum. Methods Data Syst.* **2017**, *6*, 329–343. [[CrossRef](#)]
8. Chulliat, A.; Lalanne, X.; Gaya-Piqué, L.R.; Truong, F.; Savary, J. The New Easter Island Magnetic Observatory. In *Proceedings of XIII IAGA Workshop on Geomagnetic Observatory Instruments, Data Acquisition and Processing*; U.S. Geological Survey Open File Report 2009-1226; U.S. Geological Survey: Reston, VA, USA, 2009; pp. 54–59.
9. Khomutov, S.Y.; Lingala, M. Some problems with old magnetic data processing. *E3S Web Conf.* **2020**, *19*, 602029. [[CrossRef](#)]
10. Bartels, J.; Heck, N.H.; Johnston, H.F. The three-hour-range index measuring geomagnetic activity. *J. Geophys. Res.* **1939**, *44*, 411–454. [[CrossRef](#)]
11. Janošek, M.; Butta, M.; Vlk, M.; Bayer, T. Improving Earth’s Magnetic Field Measurements by Numerical Corrections of Thermal Drifts and Man-Made Disturbances. *J. Sens.* **2018**, *2018*, 1804092. [[CrossRef](#)]
12. Curto, J.J.; Marsal, S.; Torta, J.M.; Sanclement, E. Removing spikes from magnetic disturbances caused by trains at Ebro Observatory. In *Proceedings of XIII IAGA Workshop on Geomagnetic Observatory Instruments, Data Acquisition and Processing*; Love, J.J., Ed.; U.S. Geological Survey Open File Report 2009-1226; U.S. Geological Survey: Reston, VA, USA, 2009; pp. 60–66.
13. Di Mauro, D.; Regi, M.; Lepidi, S.; Del Corpo, A.; Dominici, G.; Bagiacchi, P.; Benedetti, G.; Cafarella, L. Geomagnetic Activity at Lampedusa Island: Characterization and Comparison with the Other Italian Observatories, Including in Response to Space Weather Events. *Remote Sens.* **2021**, *13*, 3111. [[CrossRef](#)]